

Design and Analysis of a 2D Photonic Crystal-Based WDM Demultiplexer Using Cavity and Quasi-Waveguide Bend Coupling

Abdelali Boudissa

Electromagnetism and Telecommunications Laboratory, Electronics Department, University of Freres Mentouri, Constantine, Algeria

boudissa.Abdelali@umc.edu.dz (corresponding author)

Received: 29 April 2025 | Revised: 18 June 2025 | Accepted: 28 June 2025

Licensed under a CC-BY 4.0 license | Copyright (c) by the authors | DOI: <https://doi.org/10.48084/etasr.11817>

ABSTRACT

This paper proposes a four-channel demultiplexer based on 2-Dimensional Photonic Crystal (2DPC) cavities and quasi-waveguide bends for Wavelength Division Multiplexing (WDM) and examines the performance parameters of the demultiplexer, such as transmission efficiency, passband width, Q-factor, and crosstalk. The proposed demultiplexer consists of a bus waveguide, drop quasi-waveguide bends, and cavities, in which the output ports are arranged in a way that reduces channel interference or crosstalk. When simulating the performance of the device, the Finite Difference Time Domain (FDTD) approach was used and the results showed an average transmission coefficient of 91.87%, a spectral width of 0.2 nm, and an average quality factor of 7,658.5. The device achieved crosstalk levels ranging from -18.69 dB (optimal performance) to -9.262 dB (minimum performance), optimizing it for high-performance Photonic Integrated Circuits (PICs) and optical communication systems.

Keywords-photonic crystal; Wavelength Division Multiplexing (WDM) demultiplexer; cavity; Q-factor crosstalk; 2D- Finite Difference Time Domain (FDTD)

I. INTRODUCTION

Miniaturization of devices is one of the most important areas of research in optics. Photonic Crystal (PC) technology allows miniaturization of 10 to 100 times. A PC is composed of periodic dielectric materials [1] and is classified into three types: one-dimensional (1DPC), two-dimensional (2DPC), and three-dimensional (3DPC). Each has a different structure, with 1DPC exhibiting periodicity in one direction, 2DPC in two directions with homogeneity in the third, and 3DPC in all three directions. 2DPCs are widely used in the design of optical devices, with the Photonic Band Gap (PBG) being a critical factor in determining the device's operating wavelength [2]. This band gap exhibits similar behavior to the electronic band gap in semiconductor devices, controlling and manipulating light beams within photonic crystals. This paper used a square lattice structured by periodically arranging dielectric rods in an air medium. PC-based devices are designed by introducing defects into a 2DPC structure. Point and line defects are added to the design to enable light propagation within the device. Point defects create resonant cavities, and line defects form linear or bus waveguides. Defects are created by modifying structural parameter dimensions or by removing one or more rods. Many devices use 2D photonic crystals, including filters [3–7], power splitters [8], polarization splitters [9], switches [10], waveguides [11], and ring resonators [12]. These devices play a crucial role in optical communication systems by functioning as demultiplexers, which can select one or multiple

channels [13–15]. In this paper, a Wavelength Division Multiplexing (WDM) system is proposed that integrates a four-channel design within a two-dimensional photonic crystal consisting of dielectric rods in air. Each channel has a resonant cavity coupled with a quasi-waveguide bend and a line defect waveguide. The channels are arranged on both sides of the bus waveguide, creating photonic resonant cavities by varying the radius of a single rod within the photonic crystal structure. The performance of the designed WDM filter was evaluated numerically using the Finite Difference Time Domain (FDTD) method [16, 17], with Berenger's Perfectly Matched Layer (PML) surrounding the entire structure as an absorbing boundary condition [18]. The simulations yielded positive results, including high quality factors and excellent transmission efficiency, which demonstrate the advantages of this approach.

II. BASIC PHOTONIC CRYSTAL DESIGN

The study examines a 2DPC formed by a square lattice of dielectric rods within an air background. The radius of the rods is defined as $r = 0.18a$ [4], where a signifies the lattice constant [1]. The CPS-2D structure, as shown in Figure 1, comprises dielectric rods arranged in a square lattice (periodic in the x - and z -directions) with a refractive index $n=3.3763$. The 2DPC exhibits a broad photonic bandgap in the normalized frequency range $a/\lambda=0.309-0.445$ for Transverse Electric (TE) polarization [4], where λ is the free-space wavelength.

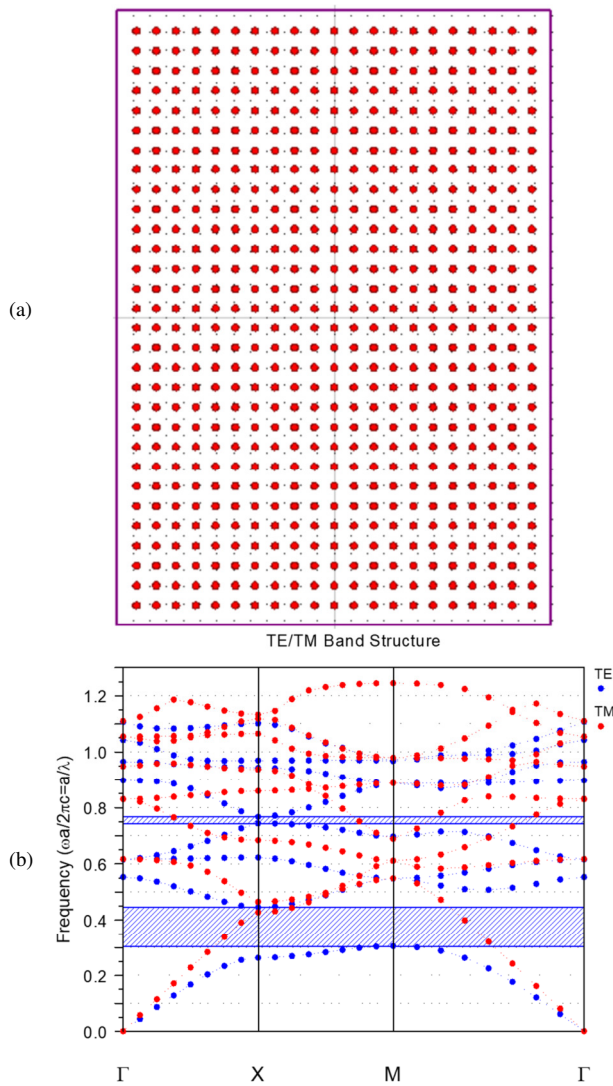


Fig. 1. (a) The schematic of a two-dimensional (2D) square-lattice photonic crystal structure, (b) photonic band structure of the 2DPC lattice without defects, computed via the PWE method.

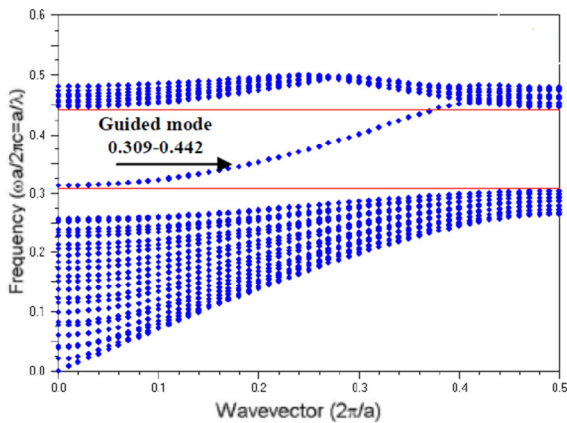


Fig. 2. Schematic of a 2DPC waveguide and the dispersion curve corresponding to defect modes within the PBG.

Figure 2 presents the photonic bandgap and the dispersion curve of the guided defect modes in the single-line-defect waveguide. A single-mode regime is observed within the normalized frequency range of 0.309 to 0.442. The 1.55- μm telecommunication window is characterized by a lattice constant a of 0.58 μm [5], which corresponds to a wavelength range of 1312 nm to 1877 nm for the defect mode, which is suitable for the design of demultiplexers for WDM applications.

III. SIMULATION AND ANALYSIS

FDTD is a numerical method that allows for the accurate propagation of electromagnetic waves through photonic crystal devices. In the proposed device, an effective and unique refractive index was used for channel selection. Consequently, the 2DFDTD [16] simulation is performed on the structures in order to obtain the output response of the typical model and the proposed demultiplexer. The grid size in the x and y directions is $a/16$, while the estimated time step (t) is set to 0.0025, and the memory size is 33.4 MB. The stability of the system can be assessed during the simulation in order to ensure that the time steps (Δt) are met and can be calculated by:

$$\Delta t \leq \frac{1}{c \sqrt{\frac{1}{\Delta x^2} + \frac{1}{\Delta z^2}}} \quad (1)$$

where c is the velocity of light and $\Delta x, \Delta z$ are the spatial steps in x - z directions. A Gaussian optical signal is applied at the base of the structures. The transmission spectra are then analyzed by performing a Fast Fourier Transform (FFT) on the electromagnetic field distribution within the system simulated by using 2D FDTD methods.

A. Typical Filter Design

The schematic of a typical photonic crystal filter is shown in Figure 3 (a), where the structure includes a cavity located between a bus waveguide and a Quasi-Waveguide Bend (QWGB). The QWGB is formed by removing a single line of L-shaped rods from the 2DPC lattice. In order to optimize light transmission into the bend, the rods labeled (a, b) are displaced by a distance of $\sqrt{2}/2 \times a$ along the Γ - M direction [19]. The waveguide's primary function is to collect signals from the cavity and direct them to the output port. The existence of a defect is confirmed by the reduction of the radius of the central cavity rod to $r=0.08a$. This setup leads to a resonant phenomenon, which emerges from the coupling interaction between the cavity and the two waveguides. Figure 3 (b) shows that the optimized transmission coefficient for a cavity radius of $r=0.08a$ attains a near-ideal transmission efficiency of $T=100\%$ and a quality factor $Q=3338$. The quality factor was calculated using the relationship $Q=\lambda_0/\Delta\lambda$ [1], where $\Delta\lambda$ is the Full Width at Half Maximum (FWHM) bandwidth of the resonance peak, and $\lambda_0=1669.1$ nm is the resonant wavelength at the center of the band.

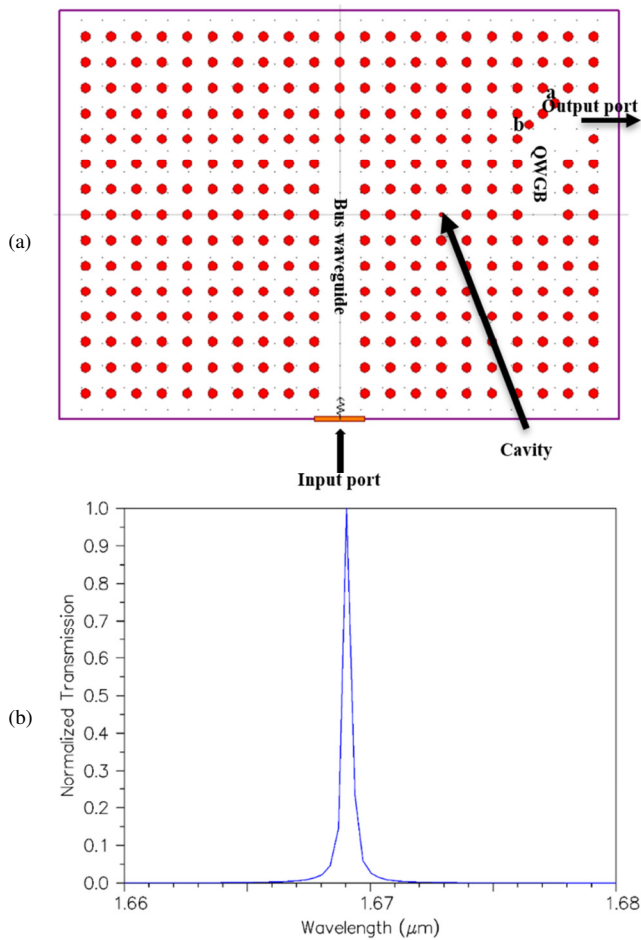


Fig. 3. (a) Schematic diagram of the typical resonator with one output port, (b) the optimized transmission response of the resonator, achieved for a cavity radius of $r = 0.08a$.

B. Design of 2DPC four-channel WDM Demultiplexer

The construction of a WDM demultiplexer is based on the optimized resonator design depicted in Figure 3(a). In order to enhance performance, the array of dielectric rods is expanded, and three additional output ports are symmetrically integrated. This reduces signal interference and crosstalk as shown in Figure 4. The demultiplexer's performance was initially examined by systematically adjusting the radius of its resonant cavities (r_1, r_2, r_3, r_4) as: $r_1=0.010a$, $r_2=0.022a$, $r_3=0.024a$, and $r_4=0.032a$. A Gaussian optical pulse, extending across the entire frequency range of interest, is generated at the input bus waveguide. Four monitors were positioned at output ports 1, 2, 3, and 4 to collect the normalized transmitted power spectral density after FFT. The pulse's input light flux traverses each cavity, where it interacts, and is subsequently detected by the monitor positioned at the output waveguide. As shown in Figure 5, the proposed WDM demultiplexer exhibits distinct output transmission spectra.

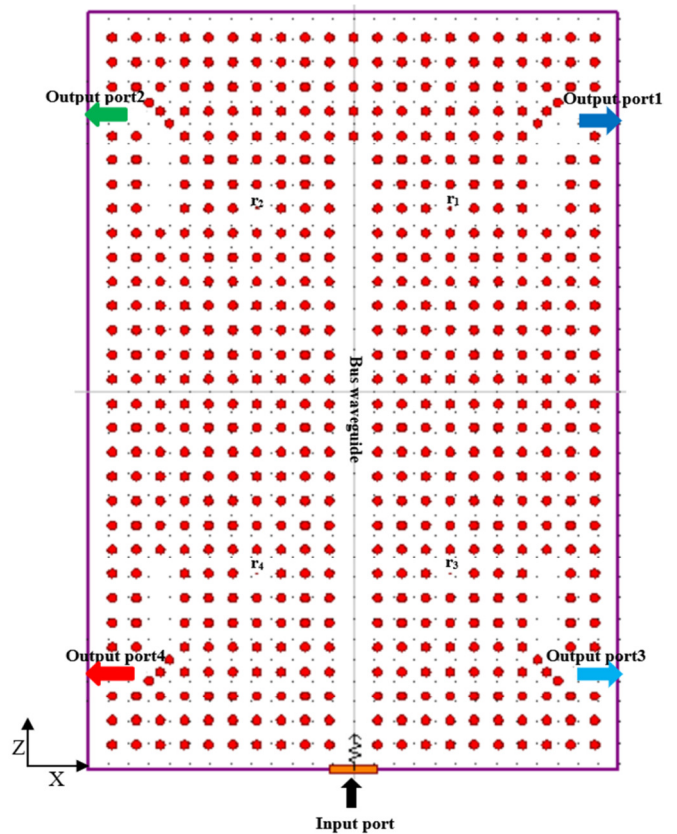


Fig. 4. Schematic structure of the proposed WDM demultiplexer.

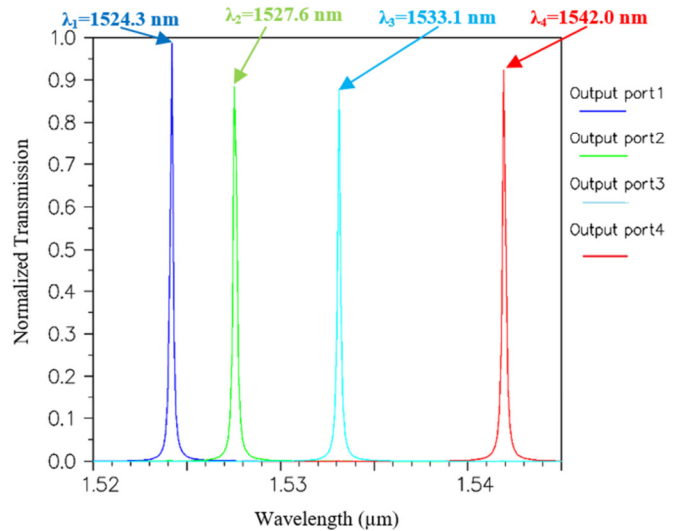


Fig. 5. The four-channel output transmission spectrum of the proposed WDM demultiplexer.

The device transmits four distinct wavelengths: 1524.3 nm (λ_1), 1527.6 nm (λ_2), 1533.1 nm (λ_3), and 1542.0 nm (λ_4), with each wavelength transmitted exclusively from its designated output port. The obtained results show channel isolation, with distinct spectral peaks corresponding to the expected wavelengths. The sharp resonance profiles with minimal channel crosstalk highlight the high spectral specificity of the

device, confirming its effectiveness for wavelength selectivity in dense photonic circuits. The operational efficiency of the demultiplexer is evaluated through the simulation of the steady-state electric field distribution for the four target wavelengths. As shown in Figure 6, the electromagnetic field profiles at the resonant wavelengths ($\lambda_1-\lambda_4$) indicate substantial modal confinement within their respective output channels. These spatial field patterns demonstrate effective wavelength-selective routing, with minimal cross-channel interference, confirming the device's ability to isolate and guide distinct spectral components to designated ports. Table I presents a synopsis of the key performance metrics of the WDM demultiplexer, including resonant wavelengths, passband widths, channel spacing, transmission efficiency, and Q-factor. The data demonstrate the device's spectral characteristics and its capacity to select and transmit distinct wavelengths with high precision. Table II summarizes the inter-channel crosstalk measurements, with the logarithmic ratio of the crosstalk power between adjacent channels to the maximum power of the neighboring channel used as the quantification method [19]. The measured crosstalk values range from -9.251 dB (maximum, indicating stronger interference) to -18.690 dB (minimum, reflecting lower interference). This level of isolation is important to ensure that signals transmitted through different channels do not interfere with each other, which is a necessary condition for high-density WDM systems. Table III provides a comparative analysis of the functional characteristics between the proposed demultiplexer and existing designs that possess the same square lattice structure and number of channels, highlighting the key performance metrics, such as the overall dimensions, number of channels, passband bandwidth, transmission efficiency, Q factor, and crosstalk levels for all four channels. Authors in [20] reported a notably high Q factor exhibiting poor transmission efficiency and a bulky design. Authors in [21] presented improved passband width and reduced crosstalk; however, its overall footprint remains substantial at $360 \mu\text{m}^2$. Authors in [22] reported that the transmission efficiency was lower and the bandwidth was wide, while authors in [12] found low crosstalk, yet its total area ($315 \mu\text{m}^2$) is considered a limitation. Authors in [23] reported a transmission efficiency of 95% and authors in [24] described a compact structure size of $180.96 \mu\text{m}^2$, a transmission efficiency of 98%, and a low Q factor. The newly designed WDM demultiplexer exhibits a surface area of $204 \mu\text{m}^2$ and an average transmission efficiency of 91.87%, along with an exceptionally high average quality factor (7658.3). These characteristics render it a potentially valuable component for photonic integrated circuits and future optical networks.

IV. CONCLUSIONS

Two-dimensional photonic crystal (2DPC)-based optical Wavelength Division Multiplexing (WDM) devices are essential for the design of Photonic Integrated Circuits (PICs), using a new configuration of a resonant defect system.

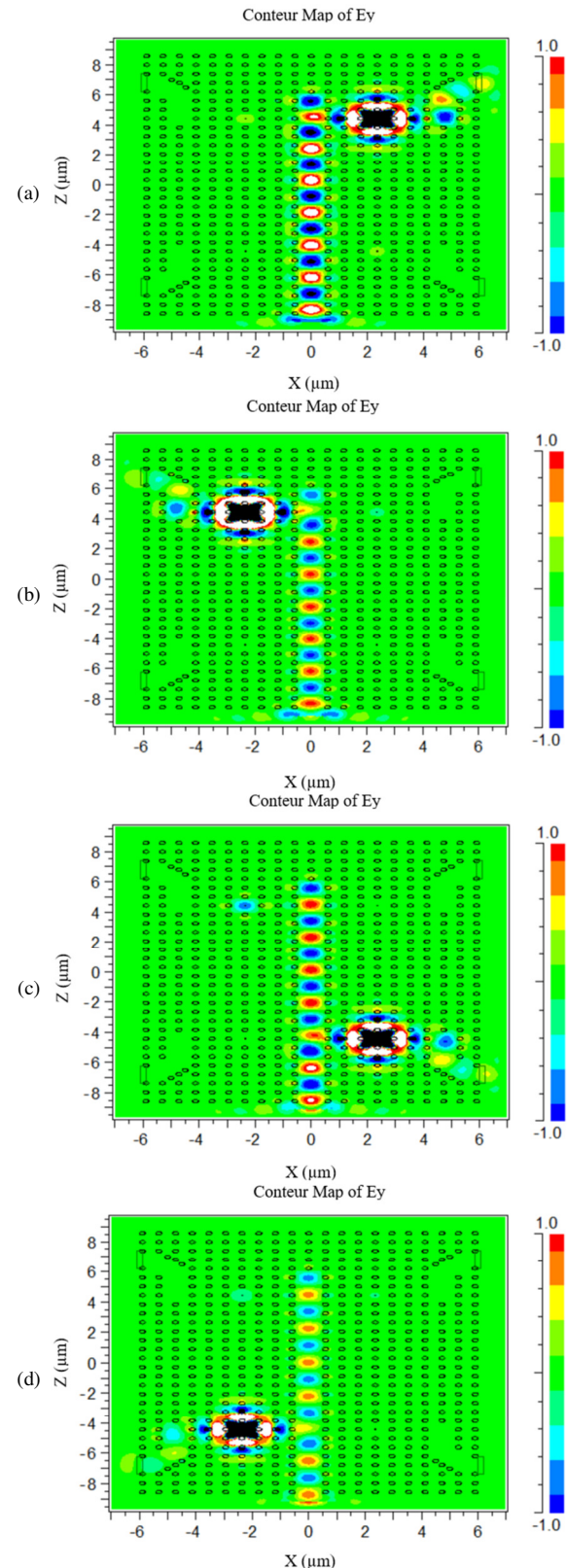


Fig. 6. The field distribution inside demultiplexer at four wavelengths: (a) $\lambda_1=1524.3$ nm, (b) $\lambda_2=1527.6$ nm, (c) $\lambda_3=1533.1$ nm, (d) $\lambda_4=1542.0$ nm.

TABLE I. PERFORMANCE CHARACTERIZATION OF THE PROPOSED WDM DEMULTIPLEXER

Output port	Resonant Wavelength (nm)	Passband Width (nm)	Channel Spacing (nm)	Transmission Efficiency (%)	Q-Factor
1	1524.3	0.2	3.3	98.62	7621
2	1527.6	0.2	5.5	88.70	7638
3	1533.1	0.2	8.9	88.15	7665
4	1542.0	0.2	8.9	92.01	7710

TABLE II. INTER-CHANNEL CROSSTALK MEASUREMENTS IN THE PROPOSED WDM DEMULTIPLEXER

Crosstalk (dB)	Output port1	Output port2	Output port3	Output port4
Output port1	-	-18.591	-18.600	-18.690
Output port2	-9.457	-	-9.468	-9.470
Output port3	-9.251	-9.261	-	-9.262
Output port4	-10.962	-10.965	-10.973	-

TABLE III. PERFORMANCE COMPARISON BETWEEN THE PROPOSED DEMULTIPLEXER AND EXISTING DESIGNS

Ref	Footprint (μm^2)	Transmission Efficiency (%)	Passband Width (nm)	Q-Factor	Largest Crosstalk (dB)
[12]	---	95	0.5	2600	-19
[20]	---	82	30	---	---
[21]	315	90	---	---	-25
[22]	484	Less than 7%	0.2	7800	---
[23]	360	93	0.4	4107	-27.33
[24]	180.96	98	0.9	1823	-3.4 to -26.9
This Study	204	91.87	0.2	7658.3	-9.251 to -18.69

The design of such structures that offer high spectral selectivity and low crosstalk remains a significant challenge. In order to address this limitation, a WDM demultiplexer based on a 2DPC structure composed of dielectric rods in air was proposed. This device uses cavity-waveguide coupling and a curved quasi-waveguide to enhance light capture and spectral resolution. The introduction of point and line defects into a photonic crystal by altering the geometric characteristics of the cavities, including the radius of the resonant cavities, has resulted in the development of a four-channel demultiplexer operating at resonant wavelengths of 1524.3 nm, 1527.6 nm, 1533.1 nm, and 1542.0 nm, occupying a compact area of 204 μm^2 . This configuration yielded an average transmission efficiency of 91.87%, a remarkably constrained spectral width of 0.2 nm, and a substantial quality factor averaging at 7658.5. The channel spacing exhibited a range from 3.3 nm to 8.9 nm, with crosstalk levels ranging from -18.69 decibels to -9.262 decibels. The findings indicate that the integration of the device into advanced optical communication networks is feasible, as evidenced by its high efficiency and minimal signal interference.

REFERENCES

- [1] J. D. Joannopoulos, S. G. Johnson, J. N. Winn, and R. D. Meade, *Photonic Crystals: Molding the Flow of Light - Second Edition*, 2nd ed. Princeton, NJ, USA: Princeton University Press, 2008.
- [2] Y. Bouazzi, N. B. Ali, H. Alsaiif, A. Boudjemline, Y. Trabelsi, and A. Torchani, "Computational Modeling of Quasi-Periodic Rudin-Shapiro Multilayered Band Gap Structure," *Engineering, Technology & Applied Science Research*, vol. 10, no. 3, pp. 5603–5607, Jun. 2020, <https://doi.org/10.48084/etasr.3455>.
- [3] J. B. Pendry, "Calculating photonic band structure," *Journal of Physics: Condensed Matter*, vol. 8, no. 9, Oct. 1996, Art. no. 1085, <https://doi.org/10.1088/0953-8984/8/9/003>.
- [4] A. Boudissa and M. Benslama, "Simulation effects of lateral coupling between L3 cavity and two quasi waveguides bends in 2D Photonic Crystal Bandpass Filter," in *2012 International Conference on Multimedia Computing and Systems*, Tangiers, Morocco, Feb. 2012, pp. 1152–1156, <https://doi.org/10.1109/ICMCS.2012.6320156>.
- [5] A. Boudissa and M. Benslama, "Designing a GaAs photonic crystals narrow band filter," *International Review of Aerospace Engineering (IREASE)*, vol. 4, no. 6, Dec. 2011.
- [6] Y. Zhou, K. Ji, W. Zhou, and H. Chen, "Design of a DWDM Multi/Demultiplexer Based on 2-D Photonic Crystals," *IEEE Photonics Technology Letters*, vol. 28, no. 15, pp. 1669–1672, Dec. 2016, <https://doi.org/10.1109/LPT.2016.2566662>.
- [7] O. El Mansouri and A. Labbani, "Analysis of a Modified Y-Branch CWDM Demultiplexer Based on Photonic Crystal Structure," *Journal of Microwaves, Optoelectronics and Electromagnetic Applications*, vol. 23, no. 1, Mar. 2024, Art. no. e2024280819, <https://doi.org/10.1590/217910742024v23i1280819>.
- [8] A. Ghaffari, F. Monifi, M. Djavid, and M. S. Abrishamian, "Analysis of Photonic Crystal Power Splitters with Different Configurations," *Journal of Applied Sciences*, vol. 8, no. 8, pp. 1416–1425, Aug. 2008.
- [9] V. Zabelin *et al.*, "Self-collimating photonic crystal polarization beam splitter," *Optics Letters*, vol. 32, no. 5, pp. 530–532, Mar. 2007, <https://doi.org/10.1364/OL.32.000530>.
- [10] Y. Wang, H. Lv, T. Jiang, and K. Zhang, "Reconfigurable optical add-drop multiplexer at 1550 nm using magnetically-coupled switches based on a photonic crystal," *Optik*, vol. 192, Sep. 2019, Art. no. 162878, <https://doi.org/10.1016/j.ijleo.2019.05.084>.
- [11] M. Khatibi Moghaddam, A. R. Attari, and M. M. Mirsalehi, "Improved photonic crystal directional coupler with short length," *Photonics and Nanostructures - Fundamentals and Applications*, vol. 8, no. 1, pp. 47–53, Jan. 2010, <https://doi.org/10.1016/j.photonics.2010.01.004>.
- [12] H. Alipour-Banaei, S. Serajmohammadi, and F. Mehdizadeh, "Optical wavelength demultiplexer based on photonic crystal ring resonators," *Photonic Network Communications*, vol. 29, no. 2, pp. 146–150, Apr. 2015, <https://doi.org/10.1007/s11107-014-0483-x>.
- [13] G. Manzacca, D. Paciotti, A. Marchese, M. S. Moreolo, and G. Cincotti, "2D photonic crystal cavity-based WDM multiplexer," *Photonics and Nanostructures - Fundamentals and Applications*, vol. 5, no. 4, pp. 164–170, Nov. 2007, <https://doi.org/10.1016/j.photonics.2007.03.003>.
- [14] V. Kannaiyan, R. Savarimuthu, and S. K. Dhamodharan, "Performance analysis of an eight channel demultiplexer using a 2D-photonic crystal quasi square ring resonator," *Opto-Electronics Review*, vol. 25, no. 2, pp. 74–79, Jun. 2017, <https://doi.org/10.1016/j.opelre.2017.05.003>.
- [15] V. R. Balaji, M. Murugan, S. Robinson, and G. Hegde, "A Novel Hybrid Channel DWDM Demultiplexer Using Two Dimensional Photonic Crystals Meeting ITU Standards," *Silicon*, vol. 14, no. 2, pp. 617–628, Jan. 2022, <https://doi.org/10.1007/s12633-020-00902-7>.
- [16] A. Taflove and S. C. Hagness, *Computational Electrodynamics: The Finite-Difference Time-Domain Method*, 3rd ed. Boston, MA, USA: Artech House Publishers, 2005.
- [17] M. Qiu and S. He, "A nonorthogonal finite-difference time-domain method for computing the band structure of a two-dimensional photonic crystal with dielectric and metallic inclusions," *Journal of Applied Physics*, vol. 87, no. 12, pp. 8268–8275, Jun. 2000, <https://doi.org/10.1063/1.373537>.
- [18] J.-P. Berenger, "A perfectly matched layer for the absorption of electromagnetic waves," *Journal of Computational Physics*, vol. 114, no. 2, pp. 185–200, Oct. 1994, <https://doi.org/10.1006/jcph.1994.1159>.
- [19] K. Sakoda, *Optical Properties of Photonic Crystals*, 2nd ed., vol. 80. Berlin, Heidelberg: Springer, 2005.
- [20] M. Djavid, F. Monifi, A. Ghaffari, and M. S. Abrishamian, "Heterostructure wavelength division demultiplexers using photonic crystal ring resonators," *Optics Communications*, vol. 281, no. 15, pp. 4028–4032, Aug. 2008, <https://doi.org/10.1016/j.optcom.2008.04.045>.

-
- [21] M. R. Rakhshani and M. A. Mansouri-Birjandi, "Heterostructure four channel wavelength demultiplexer using square photonic crystals ring resonators," *Journal of Electromagnetic Waves and Applications*, vol. 26, no. 13, pp. 1700–1707, Sep. 2012, <https://doi.org/10.1080/09205071.2012.709927>.
- [22] N. D. Gupta and V. Janyani, "Dense wavelength division demultiplexing using photonic crystal waveguides based on cavity resonance," *Optik*, vol. 125, no. 19, pp. 5833–5836, Oct. 2014, <https://doi.org/10.1016/j.ijleo.2014.07.024>.
- [23] R. Talebzadeh, M. Soroosh, and T. Daghooghi, "A 4-Channel Demultiplexer Based on 2D Photonic Crystal Using Line Defect Resonant Cavity," *IETE Journal of Research*, vol. 62, no. 6, pp. 866–872, Nov. 2016, <https://doi.org/10.1080/03772063.2016.1217175>.
- [24] V. Kannaiyan, R. Savarimuthu, and S. K. Dhamodharan, "Investigation of 2D-photonic crystal resonant cavity based WDM demultiplexer," *Opto-Electronics Review*, vol. 26, no. 2, pp. 108–115, May 2018, <https://doi.org/10.1016/j.opelre.2018.01.002>.